Rigorous Solutions of Classical Lateral Earth Pressures

J. S. Shiau*, A. V. Lyamin# and S. W. Sloan#
* The University of Southern Queensland, QLD, Australia
# The University of Newcastle, NSW, Australia

ABSTRACT: Rigorous plasticity solutions for lateral earth pressures are presented in this paper by applying advanced upper and lower bound methods. The techniques, which were developed at the University of Newcastle, use finite element formulations of the limit analysis theorems and have been successfully applied to a number of geotechnical stability analyses in the past few years. For the cases analysed in this paper, the numerical lower and upper bounds typically bracket the true limit loads to within a few percent, and are therefore useful in design practice. These accurate bounds can be computed efficiently with a standard personal computer.

INTRODUCTION

Limit analysis refers to the calculation of collapse loads and plays an important part in the practical design of many geotechnical structures. In recent years, there has been an increased geotechnical awareness of the potential benefits in using numerical limit analysis (Carter et al. 2000). Owing to the nature of many geotechnical problems, which typically involve complex geometry, inhomogeneous soil profiles and anisotropic strength characteristics, the task of estimating the ultimate load has never been an easy one. Because of its great technical importance, research on geotechnical stability analysis using advanced limit analysis techniques has long been one of the major research interests in Australia and many other countries. However, it was not until finite element formulations of the bounding theorems became available (Sloan 1988, 1989; Lyamin and Sloan 2002a,b), that the full power of limit analysis was harnessed and applications to a wide range of geotechncial structures began to grow. The development and application of numerical limit analysis methods is a major research theme of the geotechnical group at the University of Newcastle (Merifield et al. 1999; Shiau et al. 2003).

To date, limit equilibrium methods have often been used by practicing engineers to determine lateral earth pressures. Among these are the Rankine, Coulomb, and Log-spiral techniques. These limit equilibrium methods presuppose collapse is triggered by large relative movements along a predefined failure surface and that, simultaneously, the stresses on this surface reach limiting values which are governed by soil strength parameters. Once these two assumptions are made, the solution is found by invoking equilibrium and then optimising the geometry of the failure surface, either analytically or numerically, to give the lowest load. An inherent limitation of the limit equilibrium method is the need to define the general shape of the failure surface in advance, as this may affect the accuracy of the solution obtained. A typical example of this limitation is the assumption of plane failure surface in the calculation of passive resistance using Coulomb Theory. As shown by Chen (1975), it is not unusual for limit equilibrium solutions to be grossly unconservative in their estimates of the limit load, especially if the assumed form of the failure surface is physically inappropriate.

In this paper, the classical lateral earth pressure problems are investigated by using the modern limit analysis tools developed at Newcastle. Results are presented in the form of earth pressure coefficients with tables and charts provided for the purpose of design practice.

STATEMENT OF THE PROBLEM

The lateral earth pressure problem considered in this paper is illustrated in Figure 1. The back of the wall has an angle α to the horizontal and the surface of the backfill has a slope of β to the horizontal and a uniform surcharge q. In determining the passive earth resistance, a rigid retaining wall of height H is pushed horizontally into the soil. To induce active failure, the wall is allowed to move away from the backfill. The soil is taken to be c- ϕ Mohr-Coulomb material with a unit weight γ.

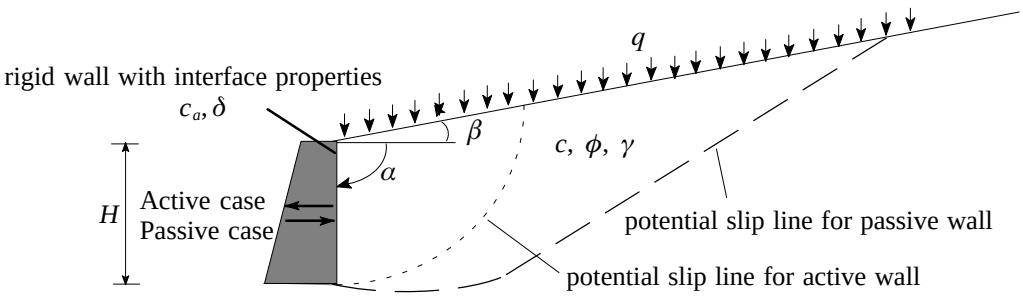

Figure 1. Problem notation and potential failure mechanisms

It is convenient to use soil-wall friction angle δ and adhesion c_a for representing the wall roughness. For a c- ϕ backfill, $\delta = 0$ and $c_a = 0$ indicates a perfectly smooth wall while a perfectly rough wall can be modelled by adopting $\delta = \phi$ and $c_a = c$. In a similar manner to the bearing capacity equation of Terzaghi, the total active and passive thrust acting on the wall, P_a and P_p, are defined in terms of earth pressure coefficients K_γ, K_c, and K_q according to

$$P_a = \frac{1}{2}\gamma H^2 K_{ar} - cHK_{ac} + qHK_{aq} \quad (1)$$

$$P_p = \frac{1}{2}\gamma H^2 K_{pr} + cHK_{pc} + qHK_{pq} \quad (2)$$

Equations (1) and (2) are governed by the geometric parameters α and β, the soil-wall friction angle δ and adhesion c_a, the surcharge q, and the backfill frictional angle ϕ. Given the above parameters, the total active and passive thrusts are computed from the finite element upper and lower bound analyses. Accordingly, the coefficients of earth pressure can be determined from the equations and are presented in this paper.

FINITE ELEMENT LIMIT ANALYSIS

A very brief summary of the finite element formulations of the upper and lower bound theorems is introduced. Detailed descriptions of the techniques can be found in Sloan (1988, 1989) and Lyamin and Sloan (2002a, 2002b).

The lower bound limit theorem states that if any equilibrium state of stress can be found which balances the applied loads and satisfies the yield criterion as well as the stress boundary conditions, then the body will not collapse. Stress fields that satisfy these requirements, and thus give lower bounds, are said to be statically admissible. The key idea behind the lower bound analysis applied here is to model the stress field using finite elements and use the static admissibility constraints to express the unknown collapse load as a solution to a mathematical programming problem. For linear stress elements, the equilibrium and stress boundary conditions give rise to linear equality constraints on the nodal stresses, while the yield condition, which requires all stress points to lie inside or on the yield surface, gives rise to a nonlinear inequality constraint on each set of nodal stresses. The objective function, which is to be maximised, corresponds to the collapse load and is a function of the unknown stresses. For linear elements, this function is also linear. After all the element coefficients are assembled, the final optimisation problem is thus one with a linear objective function, linear equality constraints and nonlinear inequality constraints.

The upper bound theorem can be formulated in terms of finite elements by adopting a similar approach to that just described for the lower bound case. This theorem states that the power dissipated by any kinematically admissible velocity field can be equated to the power expended by the external loads to give a rigorous upper bound on the true limit load. A kinematically admissible velocity field is one which satisfies compatibility, the flow rule and the velocity boundary conditions. In a finite element formulation of the upper bound theorem, the velocity field is modelled using appropriate variables and the optimum (minimum) internal power dissipation is obtained as the solution to a mathematical programming problem.

Figure 2 shows a typical finite element mesh for upper bound limit analysis of the problem considered. This mesh comprises 6765 nodes, 2349 triangular elements, and 3325 velocity discontinuities. The bottom and right hand edges of the mesh are fixed since it is assumed that the failure mechanism is contained within the proposed grid. Note that this condition needs to be checked for each case and in some instances larger meshes are necessary to ensure that the optimal failure mechanism is captured correctly. To consider the effect of soil-wall interface, those nodes on the interface boundary are given a new material property which is different from the one adopted for the backfill soil. For cohesionless soil, a smooth wall is modelled by adopting a zero interface friction angle δ. Note that the maximim value of δ is equal

to the backfill soil friction angle ϕ and representa a perfectly rough wall. To induce passive failure, an upper bound solution is obtained by prescribing a unit horizontal translation ($u = +1$) into the soil. After the resulting optimization problem is solved for the imposed boundary conditions, the upper bound on the passive forces P_p is obtained by equating the power expended by the external loads to the power dissipated internally by plastic deformation. The relevant passive earth pressure coefficients $K_{p\gamma}$, K_{pc}, and K_{pq} can then be found by direct substitution in Equations (1) and (2) .

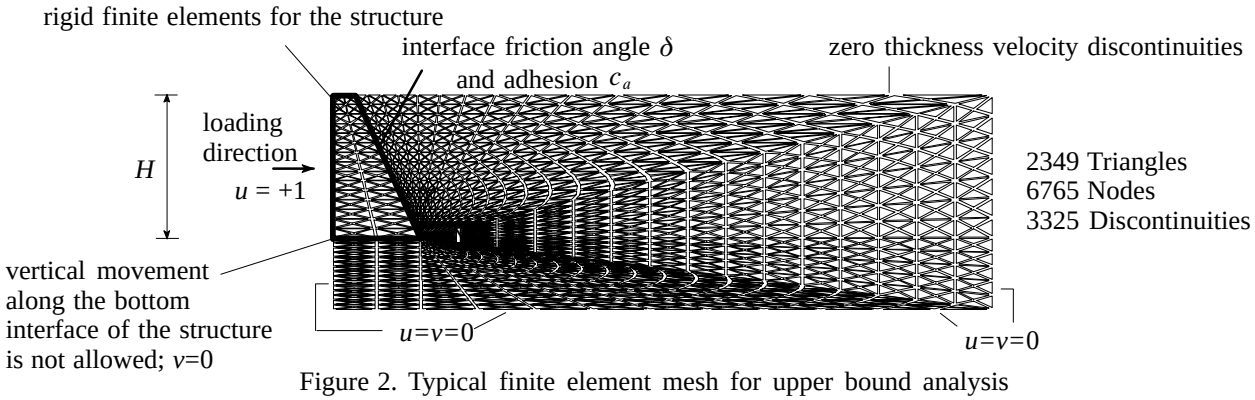

Figure 2. Typical finite element mesh for upper bound analysis ($\alpha = 60^\circ$, $\beta = 0^\circ$)

The lower bound mesh is not shown here and can be found in Shiau et al. (2004) and Lyamin et al. (2004).

RESULTS AND DISCUSSIONS

Typical Results

Numerical upper and lower bound analyses have been carried out for the case of $\phi = 35^\circ$with a vertical wall and horizontal backfill. Results for the earth pressure coefficients (K_γ, K_c, and K_q) are presented for both the active and the passive cases in Table 1 and Table 2 respectively. The various factors, K_γ, K_c, and K_q are computed by putting $c = 0$ and $q = 0$, $\gamma = 0$ and $q = 0$, and $\gamma = 0$ and $c = 0$ in the calculations respectively.

ϕ	δ/ϕ and c_a/c	K_{ar}			K_{ac}			K_{aq}		
		UB*	LB*	AVG#	UB	LB	AVG	UB	LB	AVG
35	0	0.266	0.272	0.269	1.044	1.041	1.043	0.268	0.271	0.270
	1/3	0.245	0.268	0.256	1.118	1.099	1.108	0.248	0.262	0.255
	1/2	0.241	0.260	0.251	1.167	1.147	1.157	0.244	0.258	0.251
	2/3	0.242	0.257	0.249	1.226	1.203	1.215	0.243	0.257	0.250
	1	0.247	0.261	0.254	1.387	1.360	1.373	0.249	0.269	0.259

* LB and UB : Lower and upper bound results

AVG: Averaged lower and upper bound results

Table 1. Active earth pressure coefficients from upper and lower bound analyses

Note that five sets of interface properties have been studied. For the active case, $K_{a\gamma}$ and K_{aq} decrease as the interface friction is increased, indicating that non-conservative design of an active wall can result if full friction on the soil-wall interface is assumed. It is interesting to see that the value of K_{ac} increases as the interface strengths are increased. However, this increase has an adverse effect on the total active thrust because of the negative sign in equation (1). For the passive case, $K_{p\gamma}$, K_{pc}, and K_{pq} increase as the interface strength parameters increase, indicating that the total passive resistance is increased by assuming a fully rough soil-wall interface.

ϕ	δ/ϕ and c_a/c	K_{pr}			K_{pc}			K_{pq}		
		UB*	LB*	AVG#	UB	LB	AVG	UB	LB	AVG
35	0	3.72	3.70	3.71	3.86	3.84	3.85	3.71	3.69	3.7
	1/3	5.58	5.00	5.29	6.45	5.75	6.10	5.50	5.00	5.25
	1/2	6.77	6.08	6.43	7.79	6.95	7.37	6.47	5.87	6.17
	2/3	8.17	7.32	7.74	9.12	8.29	8.70	7.45	6.85	7.15
	1	11.50	10.99	11.24	11.84	10.82	11.33	9.52	8.83	9.17

* LB and UB : Lower and upper bound results
# AVG: Averaged lower and upper bound results

Table 2. Passive earth pressure coefficients from upper and lower bound analyses

Figure 3 shows the velocity diagrams from the upper bound calculations for various values of δ/ϕ'. The plots clearly demonstrate the improved passive resistance that results from increasing the soil-wall friction and show the potential errors involved in Coulomb Theory with the assumption of plane failure surface. Interestingly, a typical Rankine solution is obtained for the smooth case ($\delta/\phi = 0$) with a planar failure surface oriented at an angle of $45^\circ - \phi/2$ to the horizontal backfill.

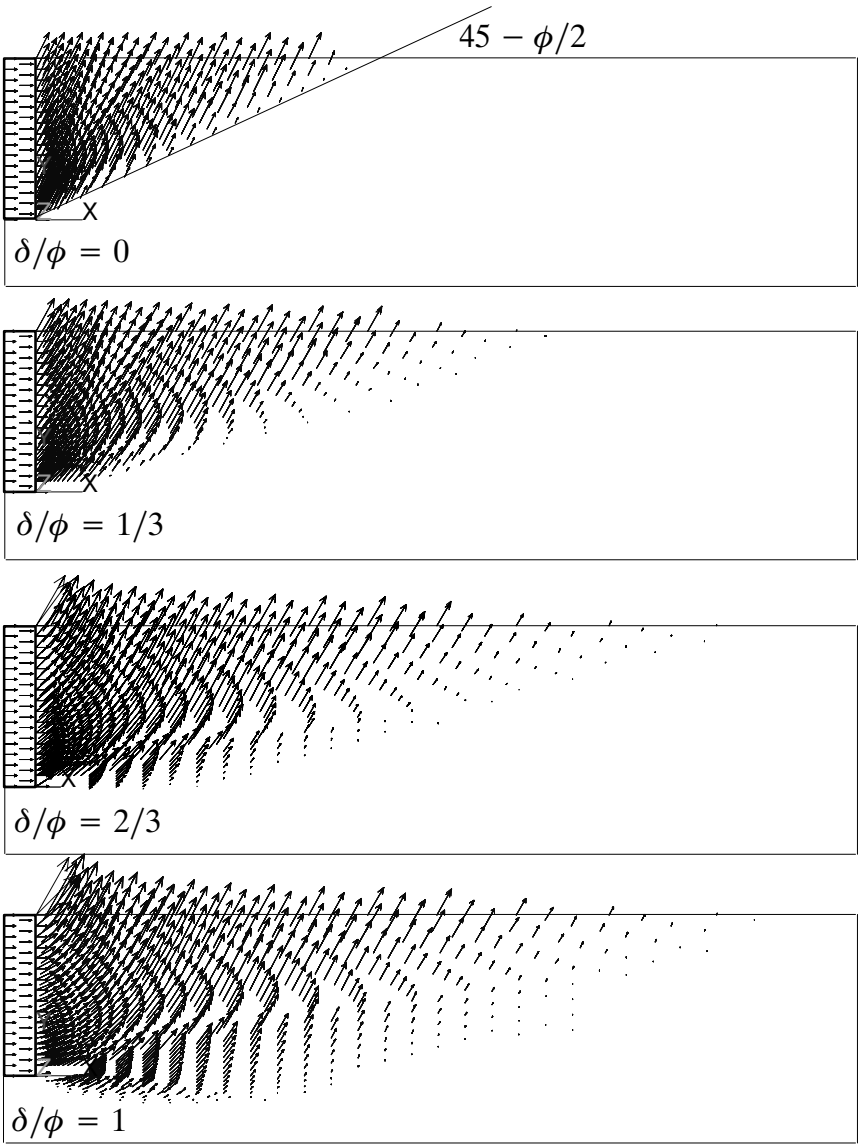

Figure 3. Velocity diagrams for various values of δ/ϕ
($\alpha = 90^\circ$, $\beta = 0^\circ$, $\phi = 35^\circ$, $c = 0$)

Note that the results presented here are for heavy walls as no vertical movement is assumed. If the weight of the wall is considered in the computation, the failure mechanism can be quite different (Shiau et al. 2004). A wide range of analyses have also been performed for passive cases with cohesionless backfill and rigorous bounding results are presented for various values of δ/ϕ in Figure 4. It is expected that any available method, based on the assumption of associated flow, should yield results which are located between our rigorous upper and lower bound solutions.

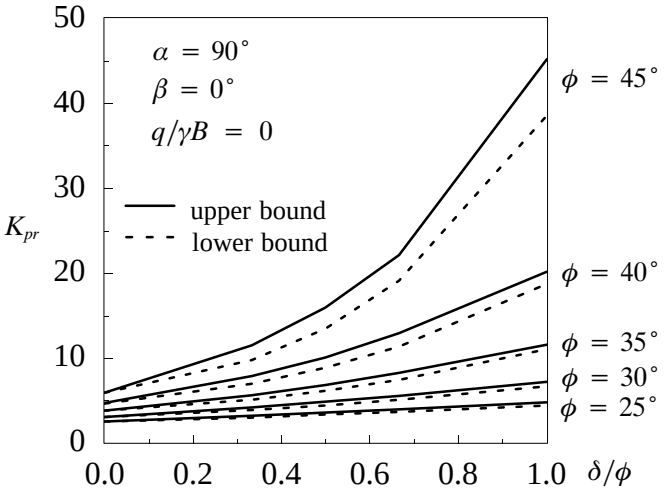

Figure 4. Typical upper and lower bound results for cohesionless backfill ($\alpha = 90^\circ$, $\beta = 0^\circ$, $c = 0^\circ$)

A Layered Example

A layered backfill has been analysed using finite element limit analysis techniques. As shown in Figure 5, The height of the wall is 6 m and the backfill consists of a drained sand overlying an undrained clay. Both perfectly smooth and perfectly rough walls are considered. For the smooth wall, the computation predicts an upper bound active thrust $(P_a)^{UB} = 166.35$ kN and a lower bound $(P_a)^{LB} = 173.21$ kN. Interestingly, hand calculation from Rankine Theory gives a value of $(P_a)^{Rankine} = 170.01$ kN.

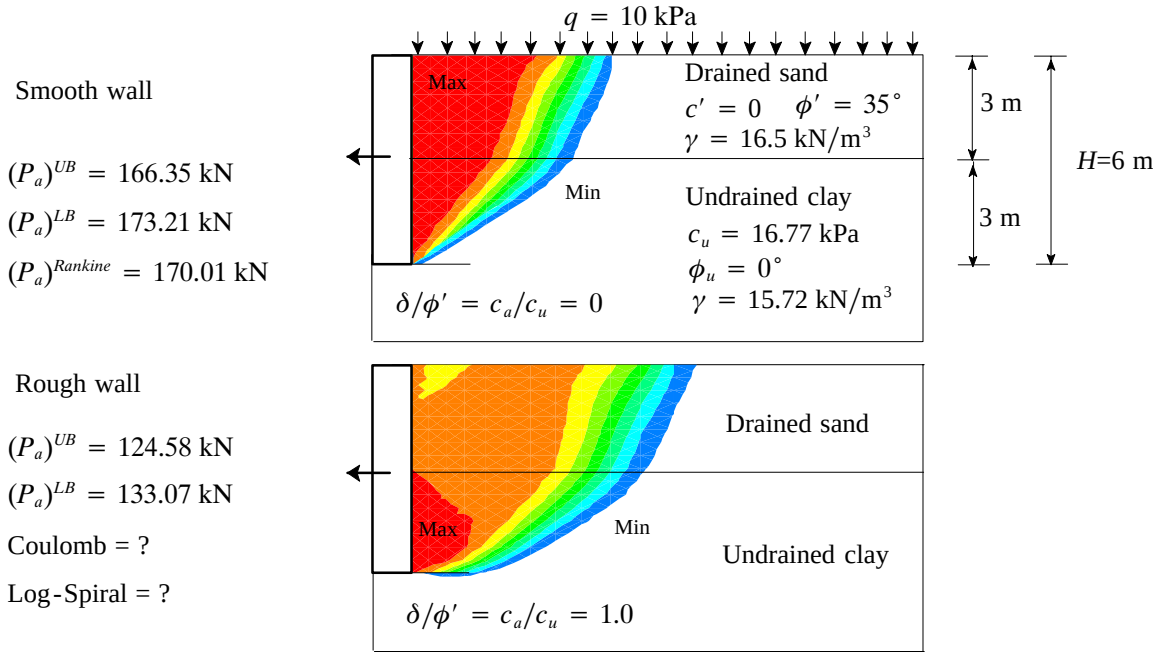

Figure 5. Velocity diagrams for active wall with smooth and rough interfaces

For the rough wall case, the upper and lower bound active thrusts were found to be $(P_a)^{UB} = 124.58$ kN and $(P_a)^{LB} = 133.07$ kN. Owing to the effect of interface friction and adhesion, the active failure mechanism for the rough case is larger than that for the smooth case, resulted in a reduction of active thrust by a factor of 1.3. On the other hand, as shown in Figure 6, the results indicate an increase of passive resistance by a factor of approximately 1.15 .

Interestingly, the boundary of the failure zone is non-planar for the active case (Figure 5), and has a complicated shape for the passive case (Figure 6). A question has thus been raised as to what is the potential error involved in using the

Coulomb method (which assumes a planar slip surface) or the log-spiral method for estimating the passive resistance of such a layered backfill. The importance of the bounding techniques can thus be easily understood from this demonstration.

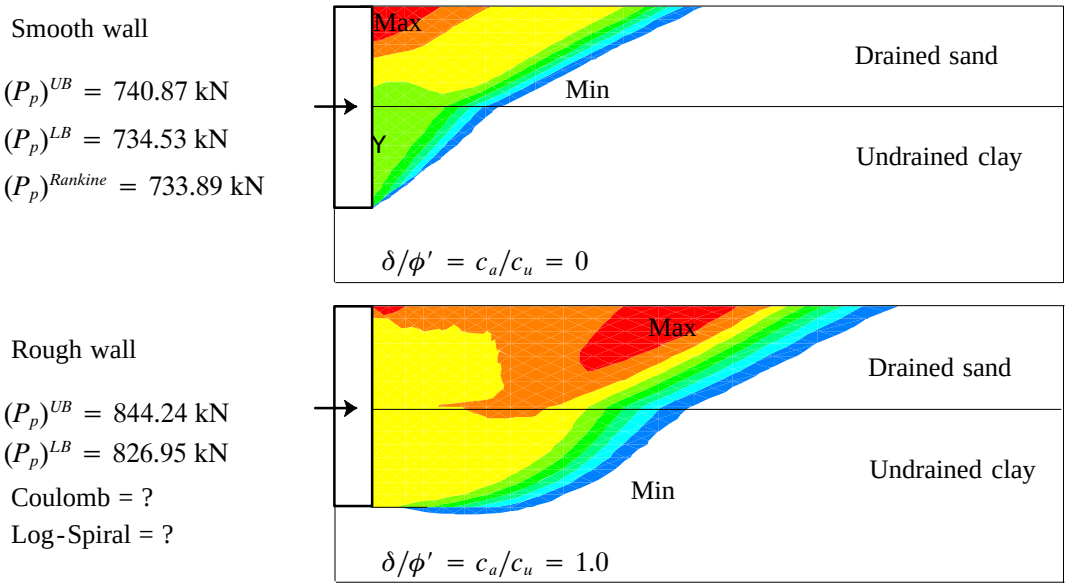

Figure 6. Velocity diagrams for passive wall with smooth and rough interfaces

CONCLUSION

The upper and lower bound solutions obtained for the active and the passive earth pressures bracket the true solution to within 10% or better. Results have been presented in the form of earth pressure coefficients with tables and charts provided for the purpose of design. It is expected that any available method, based on the assumption of associated flow, should yield results which are located between our rigorous upper and lower bound solutions. An interesting investigation regarding the velocity jumps across layered media can be made in the future.

REFERENCES

Chen, W. F. (1975). *Limit analysis and soil plasticity*, Elsevier, Amsterdam.

Carter, J. P., Desai C. S., Potts D.M., Schweiger, H.F. and Sloan, S.W. (2000). Computing and computer modelling in geotechnical engineering, Invited Paper, *GeoEng2000*, Melbourne, Australia, CD format.

Duncan, J. M and Mokwa, R. (2001). "Passive earth pressures: theories and tests." *Journal of Geotechnical and Geoenvironmental Engineering, ASCE*, 127(3), 248-257.

Lyamin, A. V. and Sloan, S. W. (2002a). "Lower bound limit analysis using nonlinear programming." *International Journal for Numerical Methods in Engineering*, 55, 573-611.

Lyamin, A. V. and Sloan, S. W. (2002b). "Upper bound limit analysis using linear finite elements and nonlinear programming." *International Journal for Numerical and Analytical Methods in Geomechanics* , 26, 181-216.

Lyamin, A. V., Shiau, J. S. and Sloan, S. W. (2004). "Calculation of active and passive earth pressure in cohesive-frictional backfills." (In preparation)

Merifield, R. S., Sloan, S. W. and Yu, H. S. (1999). "Rigorous solutions for the bearing capacity of two layered clay soils." *Géotechnique* , 49(4), 471-490.

Shiau, J. S., Lyamin, A. V. and Sloan, S. W. (2003). "Bearing capacity of a sand layer on clay by finite element limit analysis." *Canadian Geotechnical Journal*, 40, 900-915.

Shiau, J. S., Lyamin, A. V. and Sloan, S. W. (2004). "Passive earth pressure in cohesionless backfill." (To submit).

Sloan, S. W. (1988). "Lower bound limit analysis using finite elements and linear programming." *International Journal for Numerical and Analytical Methods in Geomechanics*, 12, 61-67.

Sloan, S. W. (1989). "Upper bound limit analysis using finite elements and linear programming." *International Journal for Numerical and Analytical Methods in Geomechanics*, 13, 263-282.

Terzaghi, K., Peck, R. B., and Mezri, G. (1996). *Soil mechanics in engineering practice*, 3rd Ed., John Wiley and Sons, Inc., New York.